Electronic Supplementary Material (ESI) for Journal of Materials Chemistry A.

In-situ Growth of Binder-free CNTs@Ni-Co-S Nanosheet Core/Shell Hybrids on Ni Mesh for High Energy Density Asymmetric Supercapacitors

*Tianquan Peng, Huan Yi, Peng Sun, Yuting Jing, Ruijing Wang, Huanwen Wang and Xuefeng Wang**

Shanghai Key Lab of Chemical Assessment and Sustainability, Department of Chemistry, Tongji University, Shanghai 200092, China

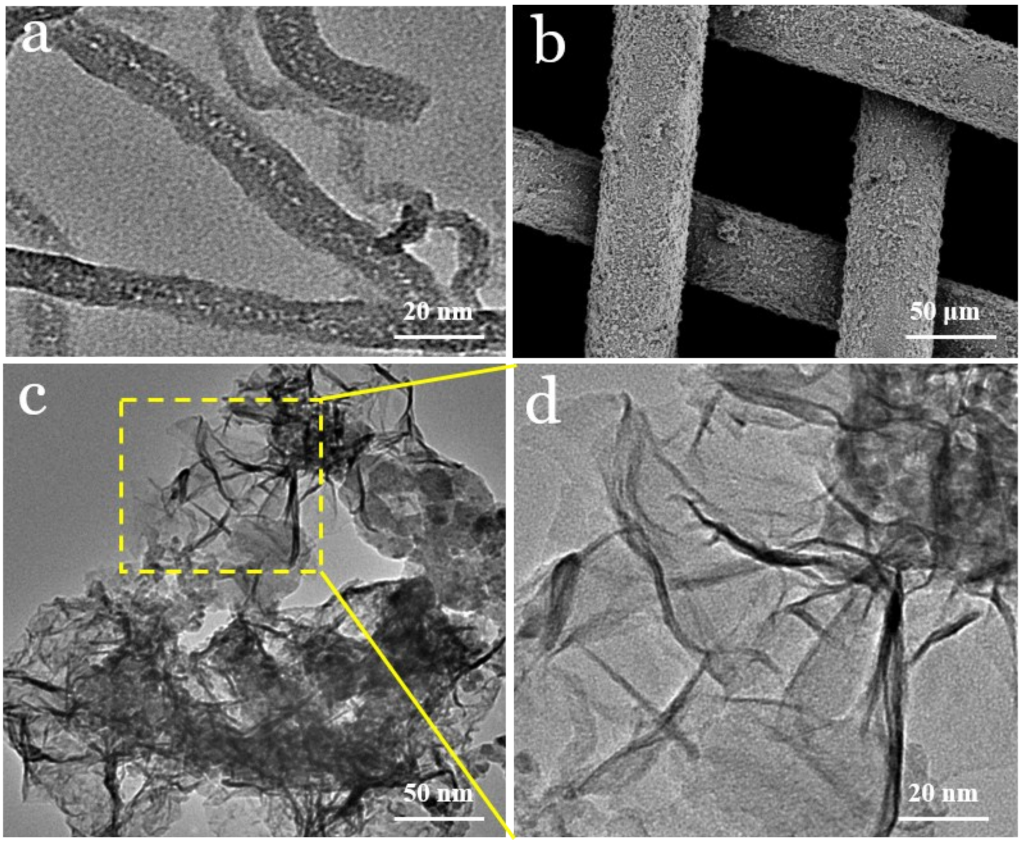

Fig. S1. (a) TEM image of the CNTs grown on Ni mesh. (b) FESEM overview images for the CNTs@Ni-Co-S composites on Ni mesh. (c-d) TEM images for Ni-Co-S nanosheets.

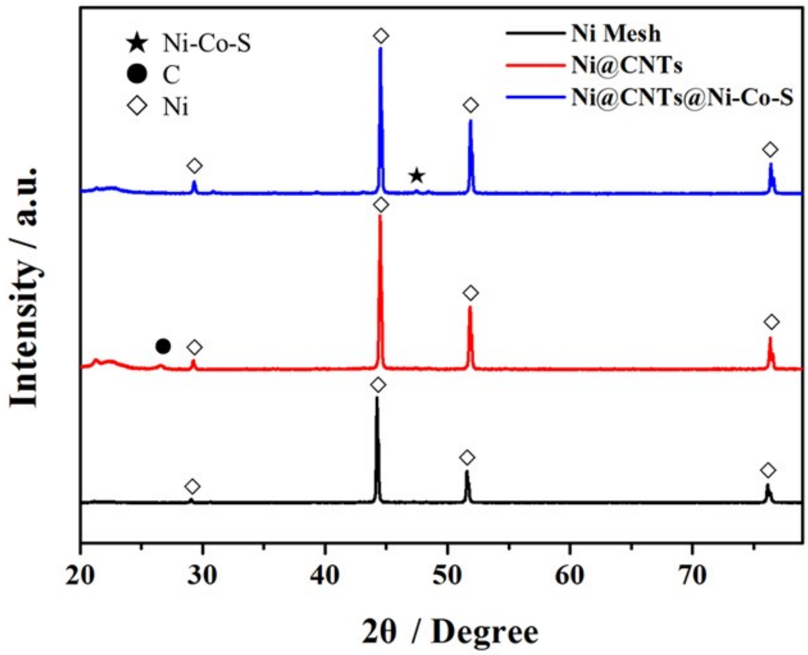

Fig. S2. The XRD patterns for Ni mesh, Ni@CNTs and Ni@CNTs@Ni-Co-S.

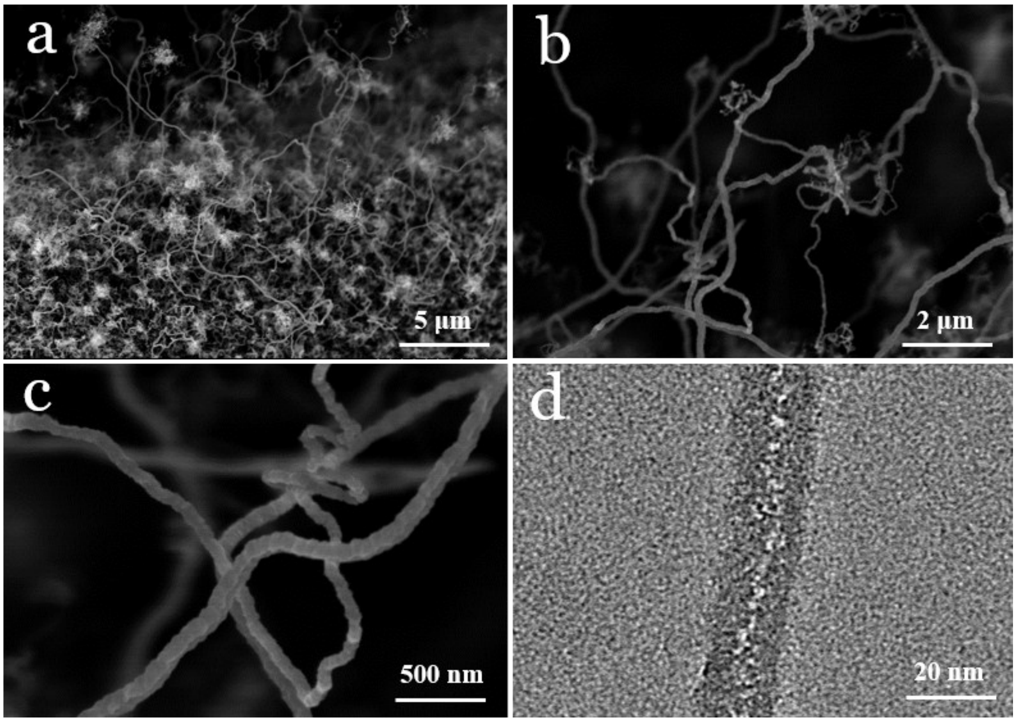

Fig. S3. (a-c) SEM images of the CNTs grown on carbon cloth. (b) TEM image for the CNTs on carbon cloth.

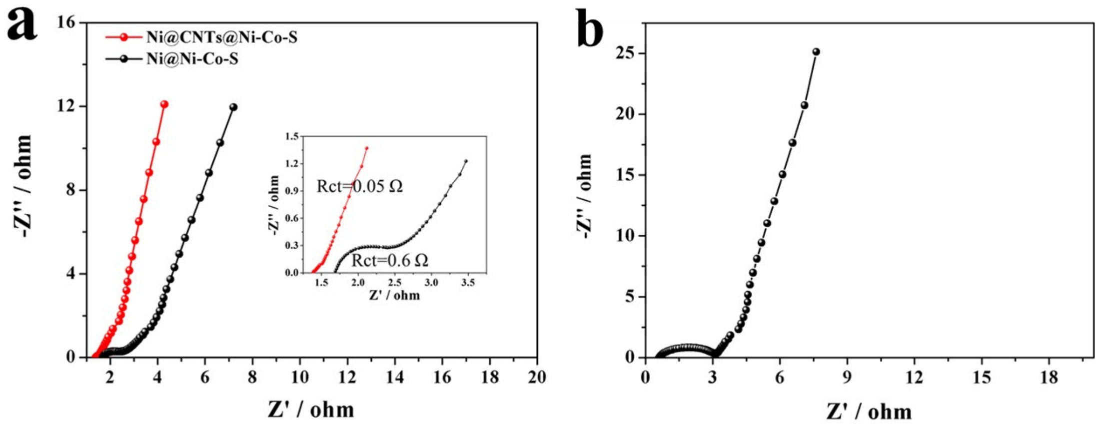

Fig. S4. Nyquist plots of (a) Ni@CNTs@Ni-Co-S and Ni@Ni-Co-S (inset: EIS spectrum in high frequency), (b) Ni@CNTs@Ni-Co-S//CC@CNTs asymmetric supercapacitors.

The Nyquist plots of Ni@CNTs@Ni-Co-S and Ni@Ni-Co-S are illustrated in Fig. S4. As shown in Fig. S4a, the axis intercepts in the high frequency range of the Ni@CNTs@Ni-Co-S is much smaller than the Ni@Ni-Co-S, indicating

Ni@CNTs@Ni-Co-S has a much smaller internal resistance (Rs). In addition, it is obvious that the semicircle of the Ni@CNTs@Ni-Co-S is much smaller than the Ni@Ni-Co-S, indicating Ni@CNTs@Ni-Co-S has a much lower interfacial charge-transfer resistance (Rct). Furthermore, Ni@CNTs@Ni-Co-S exhibits a slightly more vertical line in the low frequency range, suggesting that Ni@CNTs@Ni-Co-S has a lower Warburg resistance (described as diffusive impedance of ions) than Ni@Ni-Co-S. All the evidence show that the "core/shell" design of CNTs@Ni-Co-S composites realize a lower resistance than Ni-Co-S.

Fig. S4b illustrates the impedance data of Ni@CNTs@Ni-Co-S//CC@CNTs asymmetric supercapacitors. It can be found that the device has a low Rs ($\approx$0.6 Ω), relatively high Rct and low Warburg resistance.

Table S1. Electrochemical properties for nickel cobalt sulfide-based supercapacitors reported in recent years.

Ni-Co-S based electrode	Potential range	Specific capacitance	Rate capability	Ref.
CNTs@Ni-Co-S nanosheet core/shell arrays	-0.2 V ~ 0.6 V (vs. SCE)	222 mAh g^{-1} at 4 A g^{-1}	193 mAh g^{-1} (87.1%) at 50 A g^{-1}	this work
urchin-like $NiCo_2S_4$	0V~0.565V (vs. Hg/HgO)	180 mAh g^{-1} at 1 A g^{-1}	139 mAh g^{-1} (77.3%) at 20 A g^{-1}	1
$NiCo_2S_4$ nanosheets on graphene	0V~0.5V (vs. Ag/ AgCl)	202 mAh g^{-1} at 3 A g^{-1}	106 mAh g^{-1} (52.4%) at 20 A g^{-1}	2
$NiCo_2S_4$ porous nanotubes	-0.1V~0.5V (vs. Hg/HgO)	152 mAh g^{-1} at 0.2 A g^{-1}	76 mAh g^{-1} (50.3%) at 5 A g^{-1}	3
$NiCo_2S_4$ nanotube arrays	0V~0.55V (vs. Hg/HgO)	366 mAh g^{-1} at 5 mA cm^{-2}	248 mAh g^{-1} (67.7%) at 150 mA cm^{-2}	4
Ni-Co-S nanosheet arrays	-0.2V~0.6V (vs. Ag/ AgCl)	197 mAh g^{-1} at 5 A g^{-1}	178 mAh g^{-1} (90.6%) at 100 A g^{-1}	5
$CoNi_2S_4$/graphene nanocomposite	0V~0.38V (vs. SCE)	212 mAh g^{-1} at 1 A g^{-1}	110 mAh g^{-1} (52.1%) at 20 A g^{-1}	6
$CoNi_2S_4$ nanosheet arrays	0V~0.45V (vs. SCE)	363 mAh g^{-1} at 5 mA cm^{-2}	284 mAh g^{-1} (78.1%) at 50 mA cm^{-2}	7
Ni–Co sulfide nanowires	0V~0.45V (vs. Ag/ AgCl)	302 mAh g^{-1} at 2.5 mA cm^{-2}	147 mAh g^{-1} (48.7%) at 30 mA cm^{-2}	8
$NixCo_{3-x}S_4$ hollow nanoprisms	0V~0.5V (vs. SCE)	124 mAh g^{-1} at 1 A g^{-1}	81 mAh g^{-1} (65.4%) at 20 A g^{-1}	9
core–shell $NiCo_2S_4$ nanostructures	0V~0.5V (vs. Hg/HgO)	271 mAh g^{-1} at 1 mA cm^{-2}	215 mAh g^{-1} (79.4%) at 20 mA cm^{-2}	10
carbon@$NiCo_2S_4$ nanorods	0V~0.45V (vs. Ag/ AgCl)	182 mAh g^{-1} at 1 A g^{-1}	158 mAh g^{-1} (86.7%) at 10 A g^{-1}	11
Ni-Co-S ball-in-ball hollow spheres	-0.1V~0.55V (vs. SCE)	158 mAh g^{-1} at 1 A g^{-1}	108 mAh g^{-1} (68.1%) at 20 A g^{-1}	12
carbon-$NiCo_2S_4$ nanosheet arrays	-0.2V~0.8V (vs. SCE)	368 mAh g^{-1} at 2 mA cm^{-2}	146 mAh g^{-1} (39.6%) at 200 mA cm^{-2}	13
$NiCo_2S_4$ mesoporous nanosheets	0V~0.5V (vs. Hg/HgO)	103 mAh g^{-1} at 1 A g^{-1}	86 mAh g^{-1} (83.3%) at 20 A g^{-1}	14
$NiCo_2S_4$ nanoparticles on graphene	-0.2V~0.4V (vs. Ag/ AgCl)	190 mAh g^{-1} at 1 A g^{-1}	129 mAh g^{-1} (67.9%) at 40 A g^{-1}	15
$NiCo_2S_4$ flaky arrays	-0.1V~0.5V (vs. SCE)	284 mAh g^{-1} at 1 A g^{-1}	145 mAh g^{-1} (51.1%) at 8 A g^{-1}	16
$NiCo_2S_4$/$Ni(OH)_2$ core-shell nanotube arrays	-0.2V~0.6V (vs. Hg/HgO)	338 mAh g^{-1} at 1 mA cm^{-2}	200 mAh g^{-1} (59.3%) at 20 mA cm^{-2}	17
hollow $Ni_xCo_{9-x}S_8$ urchins@N-doped carbon	0V~0.45V (vs. Ag/ AgCl)	176 mAh g^{-1} at 2 A g^{-1}	73 mAh g^{-1} (41.3%) at 8 A g^{-1}	18

Table S2. Energy densities and power densities for nickel cobalt sulfide-based ASCs in recent reports.

Positive electrode	**Negative electrode**	**Highest potential**	**Maximum energy density**	**Maximum power density**	**Ref.**
CNTs@Ni-Co-S core/shell arrays	CNTs	1.6 V	49.2 Wh kg^{-1} (at 800 W kg^{-1})	40 kW kg^{-1} (at 18.9 Wh kg^{-1})	this work
$NiCo_2S_4$ nanotube arrays	reduced graphene oxide(RGO)	1.6 V	31.5 Wh kg^{-1} (at 156.6 W kg^{-1})	2348.5 W kg^{-1} (at 16.6 Wh kg^{-1})	4
Ni-Co-S nanosheet arrays	porous graphene film	1.8 V	60 Wh kg^{-1} (at 1.8 kW kg^{-1})	28.8 kW kg^{-1} (at 33 Wh kg^{-1})	5
$CoNi_2S_4$ nanosheet arrays	active carbon (AC)	1.7 V	33.9 Wh kg^{-1} (at 409 W kg^{-1})	2458 W kg^{-1} (at 27.2 Wh kg^{-1})	7
Ni–Co sulfide nanowires	AC	1.8 V	25 Wh kg^{-1} (at 447 W kg^{-1})	3.57 kW kg^{-1} (at 17.8 Wh kg^{-1})	8
porous Ni-Co sulphides	RGO	1.6 V	37.6 Wh kg^{-1} (at 775 W kg^{-1})	23.25 kW kg^{-1} (at 17.7 Wh kg^{-1})	19
core–shell $NiCo_2S_4$ nanostructures	porous carbon	1.6 V	22.8 Wh kg^{-1} (at 160 W kg^{-1})	2.47 kW kg^{-1} (at 10.6 Wh kg^{-1})	10
2D porous Ni-Co Sulfide	AC	1.8 V	41.4 Wh kg^{-1} (at 414 W kg^{-1})	4.8 kW kg^{-1} (at 23.8 Wh kg^{-1})	20
$NiCo_2S_4$ nanosheets	FeOOH nanorods	1.6 V	45.9 Wh kg^{-1} (at 1.7 kW kg^{-1})	8.6 kW kg^{-1} (at 19.9 Wh kg^{-1})	21
Ni-Co-S ball-in-ball hollow spheres	graphene/ carbon spheres	1.6 V	42.3 Wh kg^{-1} (at 476 W kg^{-1})	10.2 kW kg^{-1} (at 22.9 Wh kg^{-1})	12
carbon-$NiCo_2S_4$ nanosheet arrays	AC	1.8 V	68.82 Wh kg^{-1} (at 47.83 W kg^{-1})	1.4 kW kg^{-1} (at 26.74 Wh kg^{-1})	13
$NiCo_2S_4$ mesoporous nanosheets	AC	1.6 V	25.5 Wh kg^{-1} (at 334 W kg^{-1})	8 kW kg^{-1} (at 10.8 Wh kg^{-1})	14
3D cauliflower-like $NiCo_2S_4$ architectures	AC	1.6 V	44.8 Wh kg^{-1} (at 401 W kg^{-1})	16 kW kg^{-1} (at 23.1 Wh kg^{-1})	22
graphene@$NiCo_2S_4$ nanoparticles	AC	1.7 V	68.5 Wh kg^{-1} (at 850 W kg^{-1})	17 kW kg^{-1} (at 37.7 Wh kg^{-1})	15
mesoporous $NiCo_2S_4$ nanoparticles	AC	1.5 V	28.3 Wh kg^{-1} (at 245 W kg^{-1})	9.8 kW kg^{-1} (at 6.8 Wh kg^{-1})	23

Table S3. Energy densities comparison calculated via two different methods

Current density ($A\ g^{-1}$)	**1**	**2**	**4**	**8**	**10**	**15**	**20**	**30**	**40**	**50**
$E = I\int_{t=0}^{t=t} V(t)\,dt$ ($Wh\ kg^{-1}$)	46.5	42.1	38.9	35.3	34.2	29.8	26.4	21.1	17.4	15.9
$E=0.5C_s\Delta V^2/3.6$ ($Wh\ kg^{-1}$)	49.2	45.6	41.9	37.9	34.4	31.0	28.9	22.0	19.6	18.9

References

1. H. Chen, J. Jiang, L. Zhang, H. Wan, T. Qi and D. Xia, *Nanoscale*, 2013, 5, 8879-8883.
2. S. Peng, L. Li, C. Li, H. Tan, R. Cai, H. Yu, S. Mhaisalkar, M. Srinivasan, S. Ramakrishna and Q. Yan, *Chem. Commun.* , 2013, 49, 10178-10180.
3. H. Z. Wan, J. J. Jiang, J. W. Yu, K. Xu, L. Miao, L. Zhang, H. C. Chen and Y. J. Ruan, *Crystengcomm*, 2013, 15, 7649-7651.
4. H. Chen, J. Jiang, L. Zhang, D. Xia, Y. Zhao, D. Guo, T. Qi and H. Wan, *J. Power Sources* 2014, 254, 249-257.
5. W. Chen, C. Xia and H. N. Alshareef, *Acs Nano*, 2014, 8, 9531-9541.
6. W. Du, Z. Wang, Z. Zhu, S. Hu, X. Zhu, Y. Shi, H. Pang and X. Qian, *Journal of Materials Chemistry A*, 2014, 2, 9613.
7. W. Hu, R. Chen, W. Xie, L. Zou, N. Qin and D. Bao, *ACS Appl. Mat. Interfaces* 2014, 6, 19318-19326.
8. Y. Li, L. Cao, L. Qiao, M. Zhou, Y. Yang, P. Xiao and Y. Zhang, *Journal of Materials Chemistry A*, 2014, 2, 6540.
9. L. Yu, L. Zhang, H. B. Wu and X. W. Lou, *Angewandte Chemie-International Edition*, 2014, 53, 3711-3714.
10. W. Kong, C. C. Lu, W. Zhang, J. Pub and Z. H. Wang, *Journal of Materials Chemistry A*, 2015, 3, 12452-12460.
11. L. Li, Z. Dai, Y. Zhang, J. Yang, W. Huang and X. Dong, *RSC Advances*, 2015, 5, 83408-83414.
12. L. Shen, L. Yu, H. B. Wu, X.-Y. Yu, X. Zhang and X. W. Lou, *Nature Communications*, 2015, 6.
13. H. Wang, C. Wang, C. Qing, D. Sun, B. Wang, G. Qu, M. Sun and Y. Tang, *Electrochim. Acta* 2015, 174, 1104-1112.
14. Z. Wu, X. Pu, X. Ji, Y. Zhu, M. Jing, Q. Chen and F. Jiao, *Electrochim. Acta* 2015, 174, 238-245.
15. Y. Xiao, D. Su, X. Wang, L. Zhou, S. Wu, F. Li and S. Fang, *Electrochim. Acta* 2015, 176, 44-50.
16. Z. H. Yang, X. Zhu, K. Wang, G. Ma, H. Cheng and F. F. Xu, *Appl. Surf. Sci.* ,

2015, 347, 690-695.
17. J. Zhang, H. Gao, M. Y. Zhang, Q. Yang and H. X. Chuo, *Appl. Surf. Sci.* , 2015, 349, 870-875.
18. Y. Zhang, C. Sun, H. Su, W. Huang and X. Dong, *Nanoscale*, 2015, 7, 3155-3163.
19. H. Chen, J. Jiang, Y. Zhao, L. Zhang, D. Guo and D. Xia, *Journal of Materials Chemistry A*, 2015, 3, 428-437.
20. X. Li, Q. Li, Y. Wu, M. Rui and H. Zeng, *ACS Appl. Mat. Interfaces* 2015, 7, 19316-19323.
21. Y. Li, M. Zhou, X. Cui, Y. Yang, P. Xiao, L. Cao and Y. Zhang, *Electrochim. Acta* 2015, 161, 137-143.
22. Y. Xiao, Y. Lei, B. Zheng, L. Gu, Y. Wang and D. Xiao, *Rsc Advances*, 2015, 5, 21604-21613.
23. Y. Zhu, Z. Wu, M. Jing, X. Yang, W. Song and X. Ji, *J. Power Sources* 2015, 273, 584-590.